Prospettive future dell'imaging in Medicina Nucleare ed attività di Fisica Medica nel settore

Prof. Roberto Pani

Facoltà di Farmacia e Medicina - INFN Roma1

Dip. Medicina Molecolare Sapienza Università di Roma

What is emission tomography?

- Nuclear imaging techniques,based on the detection of photons in vivo, emitted by a radio-tracer injected into the patient.
- Diagnostic radiopharmaceuticals or tracers reflect physiological function with limited anatomical information

- Two different techniques:
  - **Single Photon Emission Tomography (SPECT):**

    a tracer molecule is labelled with single γ-emitting radionuclides. (Tc99m)
  - **Positron Emission Tomography (PET):**

    a tracer molecule is labelled with positron-emitting radionuclides (18F, 11C).

Relation To Anatomic Imaging

Person alive | **Person dead**

MRI scan

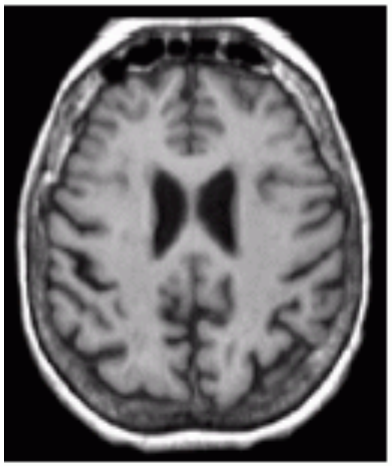

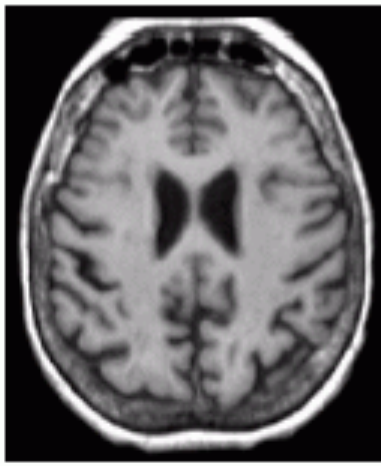

Anatomical imaging

PET scan

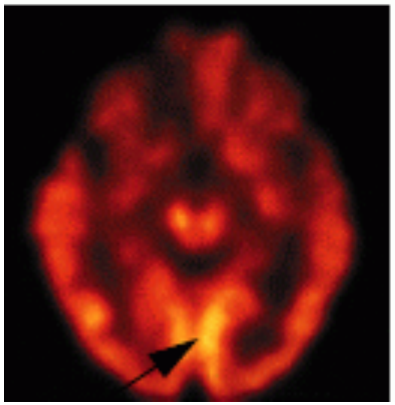

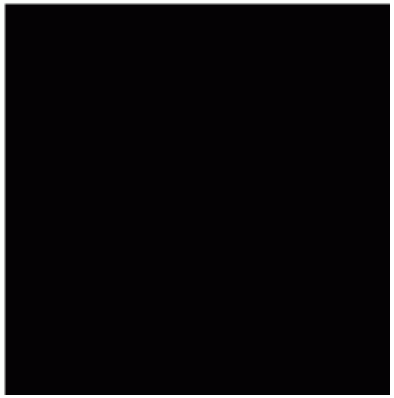

Funtional imaging

An MRI/CT scan shows you that you have a brain
A PET/SPET scan shows that you use it

Courtesy of Klaus Mueller Computer Science Department Stony Brook University

SPET basic physics

ANGER CAMERA: “Single Photon” Imaging

1. Housing
2. Pb shield
3. Collimator
4. NaI(Tl) planar crystal
5. PMT matrix

Anger Camera:
Total body scan

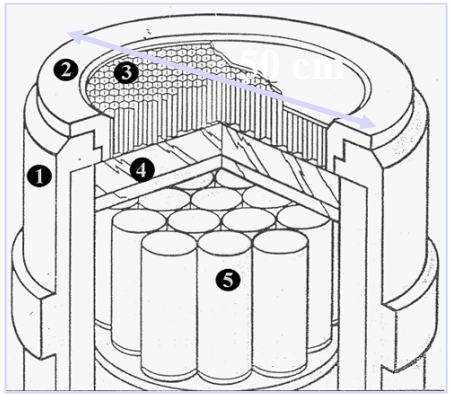

Positioning

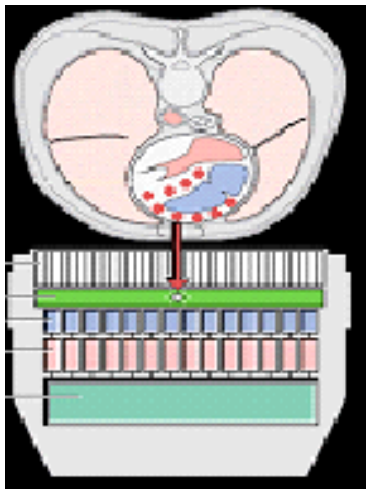

Imaging

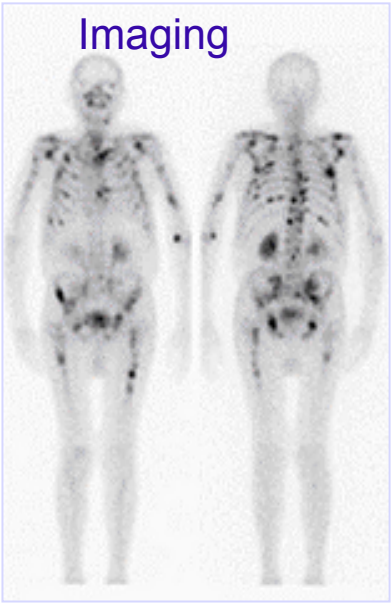

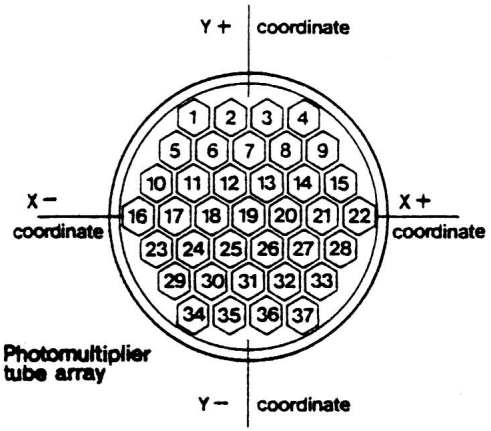

Summing matrix circuit

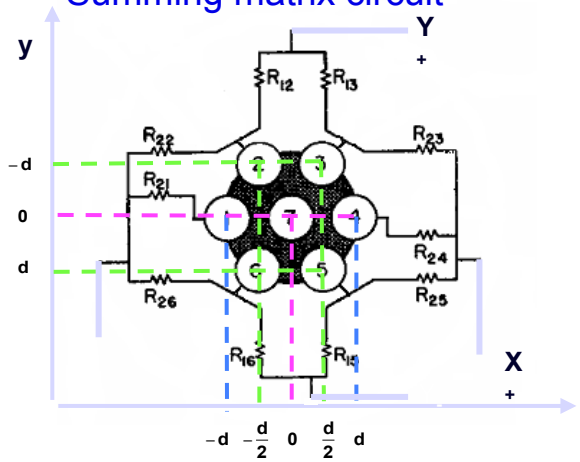

Position determination:

$$X=(x^{+}-x^{-})/(x^{+}+x^{-})$$

$$Y=(y^{+}-y^{-})/(y^{+}+y^{-})$$

Motivation for the development of new cameras

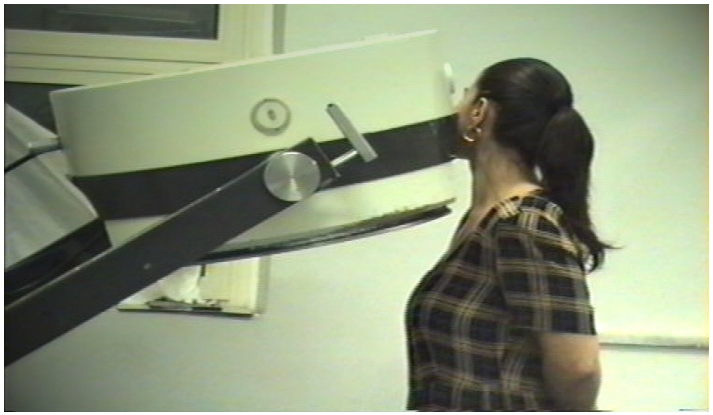

Inability for close-proximity imaging
limited spatial resolution
limited sensitivity

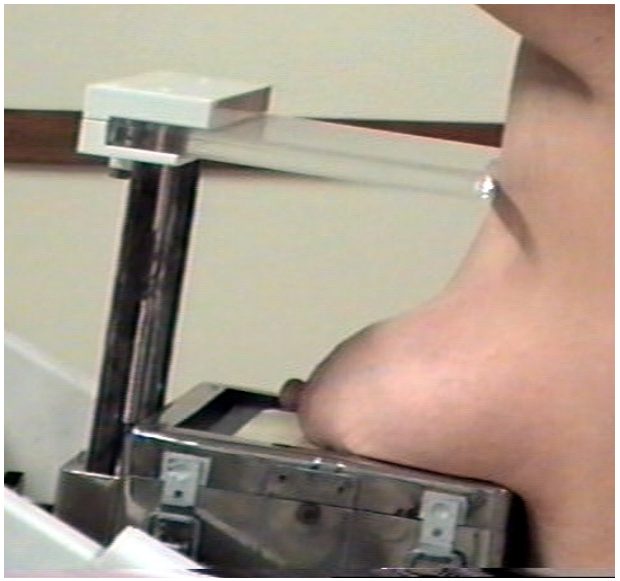

Scintimammography

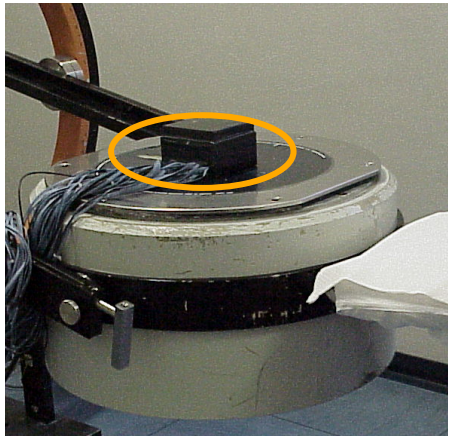

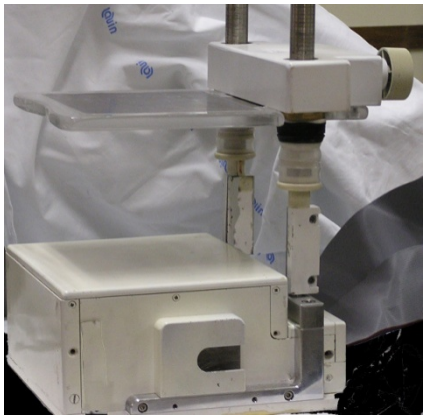

Dedicated gamma camera

Latest generation gamma cameras

http://www.digirad.com

Discrete CsI(Tl)-SiPD Detectors
Individual readout
Low noise electronics
20 x 20 cm^2 FoV

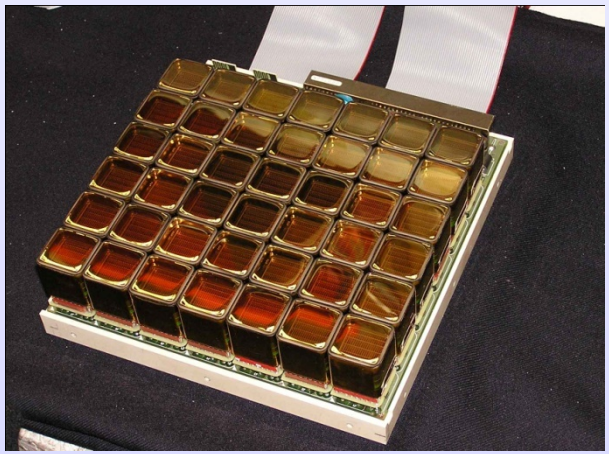

Multi-PSPMT NaI(Tl) pixellated 1st generation gamma camera 18x16 cm^2(2001)

INFN-IMI project
Pol.Hi.Tech -CAEN

Pixellated CdZnTe 2nd generation Gamma Camera 12.5 x12.5 cm^2 (2005)

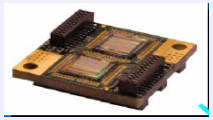

Gamma Medica Ideas Inc., Northridge, California, USA

latest generation cameras performances

Camera	Material	Pixel size (mm)	Intrinsic Spatial Resolution (mm)	Detector sensitivity (%)	Total Spatial Resolution (mm) @ 5 cm	Sensitivity (Cts/min/μCi)	Energy Resolution (%)	Tumor Visibility Score (1÷10)	Tumor SNR LEHR
Helix Helscint Anger camera	NaI(Tl)	---	3.5	100.0	6.7	90 (LEHR)	8.7	3.6	2
Gamma Medica Lumagen	CZT	1.5	1.5	52.0	9.0	370 (LEAP-HS)	6.5	5.6	3
General Electric Prototype	CZT	2.5	2.5	58.5	5.0	320 (Matched Short Bore AP)	9.0	4.4	4
Digirad 2020tc	CsI(Tl)	3.0	3.0	67.5	5.5	335 (LEAP)	11.0	6.0	6
Dilon Technologies LLC	NaI(Tl)	3.0	3.0	70.0	10.0	370 (LEHS)	18.0	N.A	N.A
IMI Multi PSPMT	NaI(Tl)	1.8	1.8	62.3	5.5	350 (LEAP)	12.0	5.6	6

All cameras have a FoV between 16 x 18 cm^2 and 20 x 20 cm^2

Advantages of Compact Gamma Cameras

Anger Camera

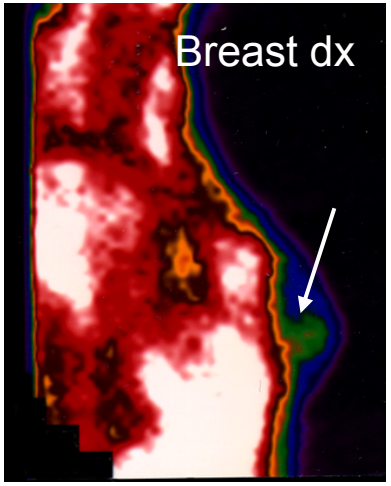

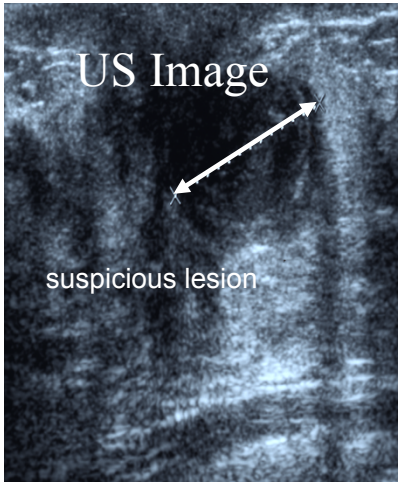

99mTc MIBI Scintimammography

Dedicated gamma camera

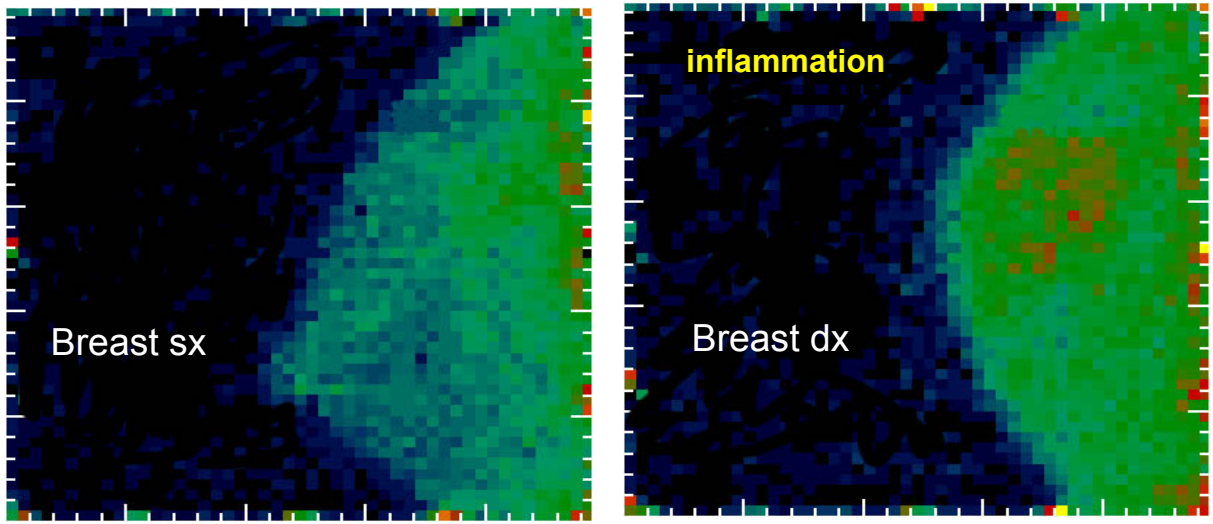

42 PSPMTs camera – NaI(Tl)

High Resolution Scintimammography helps in differentiating benign from malignant finding in scintigraphic hot spot

$LaBr_3$:Ce : latest generation of scintillation crystals

	E (keV)	Density (g/cm^3)	Atten.len. (mm)	$Z_{eff.}$	Photo-fraction (%)	Light yield (*ph*/MeV)	Decay time (ns)	Refr. index	ΔE/E (PMT)	Emiss max (nm)
CsI(Tl)	140	4.51	2.55	52.0	86	66,000	630	1.80	14%	565
$LaBr_3$:Ce	140	5.07	3.32	47.4	79	63,000	16 (97%)	1.90	6%	380
NaI:Tl	140	3.67	3.76	51.0	84	38,000	230	1.85	9%	410

Light Yield vs Energy

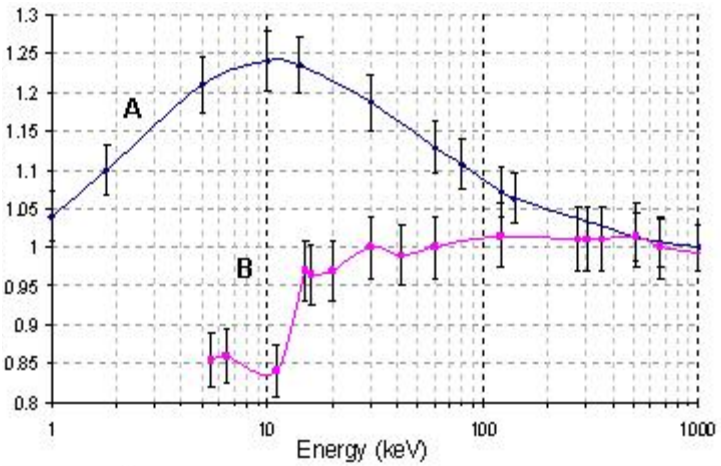

[A] – *Prescott and Narayan, NIM A, 75 (1969)*
[B] – *G.Bizarri, IEEE TNS, Vol 53,02 (2006)*

Energy Resolution

$$R^2(E) = R_s^2 + \frac{5.56}{\bar{N}\eta\alpha}\left(\frac{\delta}{\delta - 1}\right)$$

Crystal	ER(%) @ 662 keV	$ER_{scint.}$ (%)	ER_{st} (%)	Ref.
NaI(Tl)	6.7	5.9	3.2	typical
CsI(Tl)	6.6	5.8	3.2	Allier (1998)
$LaBr_3$(Ce)	3.6	2.2	2.5	Moszynski (2006)

LaBr:Ce can solve limitations offered by segmented detectors

"Mario" transmission Pb mask Co57 flood field irradiation

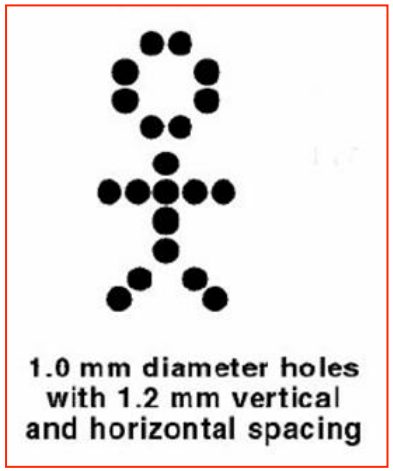

CsI(Tl) 4x4 array
1.2 mm pixel

CZT crystal
Medipix II

INFN Napoli (P. Russo)

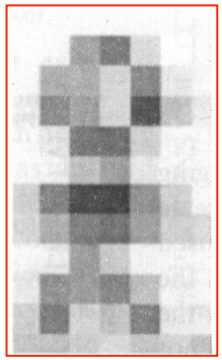

CsI(Tl) 4x4 array
1.2 mm pixel

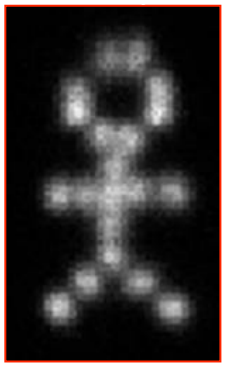

$LaBr_3$:Ce 5 mm thickness

Spatial Resolution = 0.90 mm

Efficiency: 80%

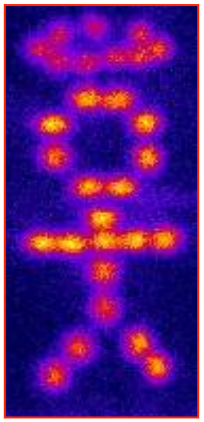

$LaBr_3$:Ce 1.5 mm thickness

Spatial Resolution = 0.65 mm

Efficiency: 35%

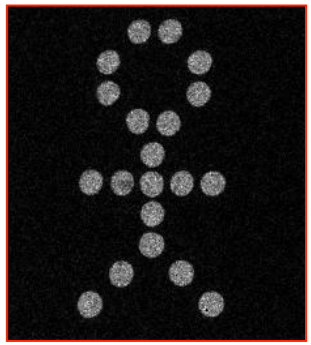

50 μm pixel

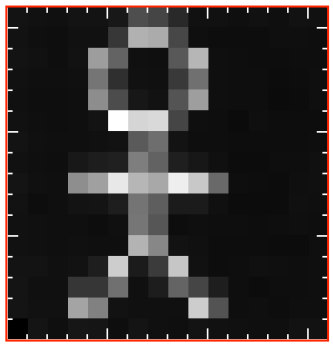

800 μm pixel

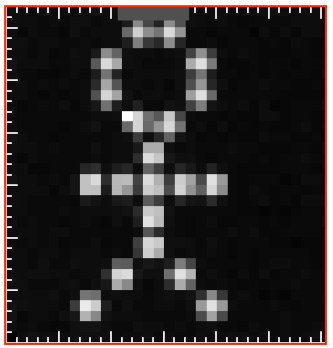

400 μm pixel

Towards Radiological Spatial Resolution

NaI(Tl) 1.5 mm thick integral assembly

Hamamatsu H8500

Tc^{99m} flood field irradiation of parallel-hole Collimator

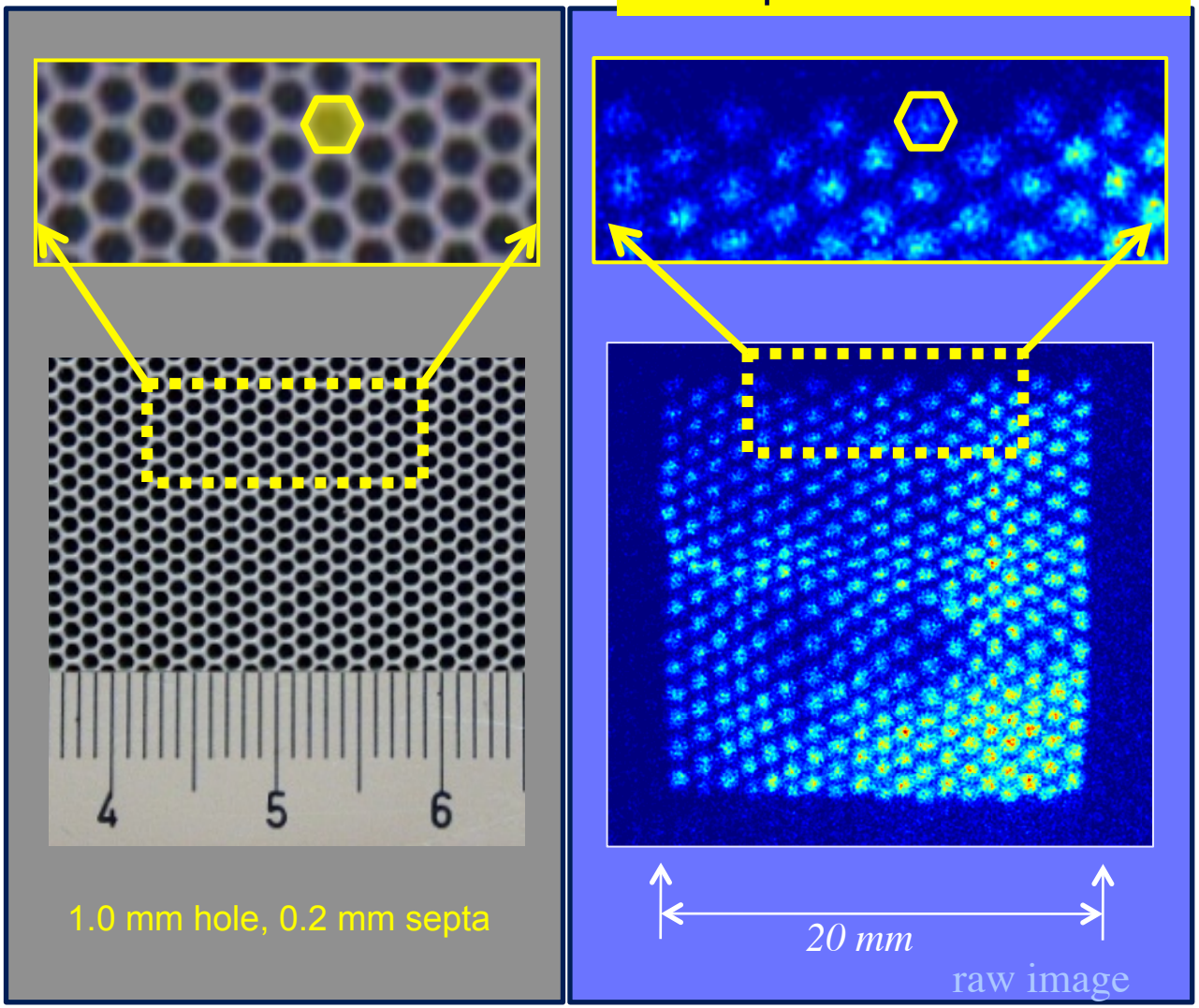

Towards Radiological Spatial Resolution

	NaI(Tl) continuous		NaI(Tl) array
Energy (keV)	SR tot (*) (mm)	SR intr. (mm)	Pixel ID (mm)
30	0.75	0.63	0.54
80	0.60	0.45	0.39
140	0.53	0.35	0.35
356	0.48	0.26	0.22
662	-	-	0.19

(*) 0.4 mm Collimated source

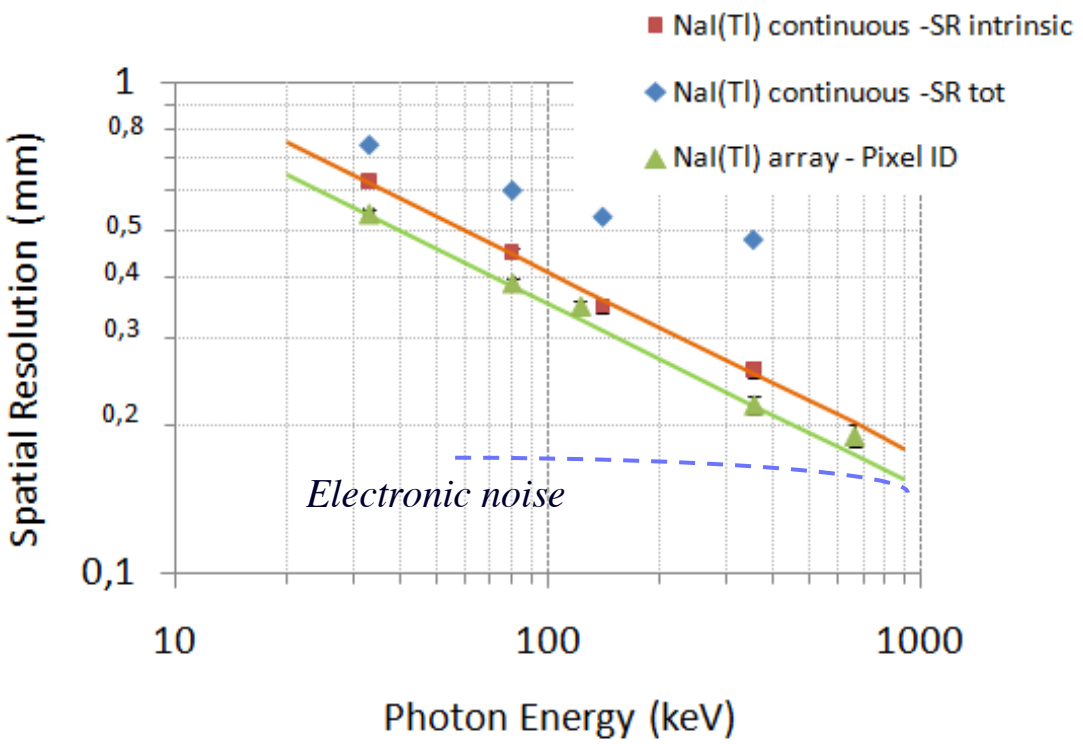

- Very low noise contribute to SR (<0.15 mm)
- SR close to the statistical limit for both crystals
- Impressive SR results in the whole Energy range

PET principle

- A β^+ emitting radiotracer is injected to a "patient"
- The radiotracer marks a specific function (e.g. glucose metabolism) - Uptake process
- The positron annihilates with an electron and two nearly collinear 511keV photons are emitted simultaneously in opposite direction.

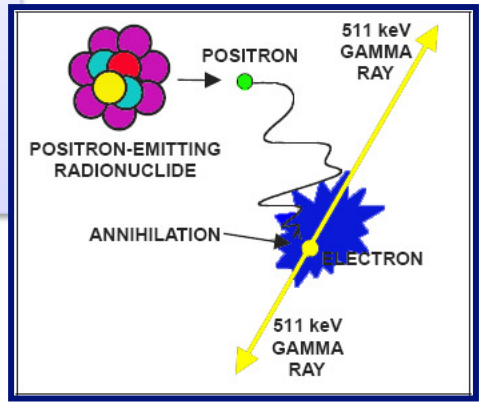

PET detectors detect the "back-to-back" photons 511 keV produced during the annihilation process

Ring geometry (stationary)

Parallel plane geometry (180° rotation)

PET Count rate

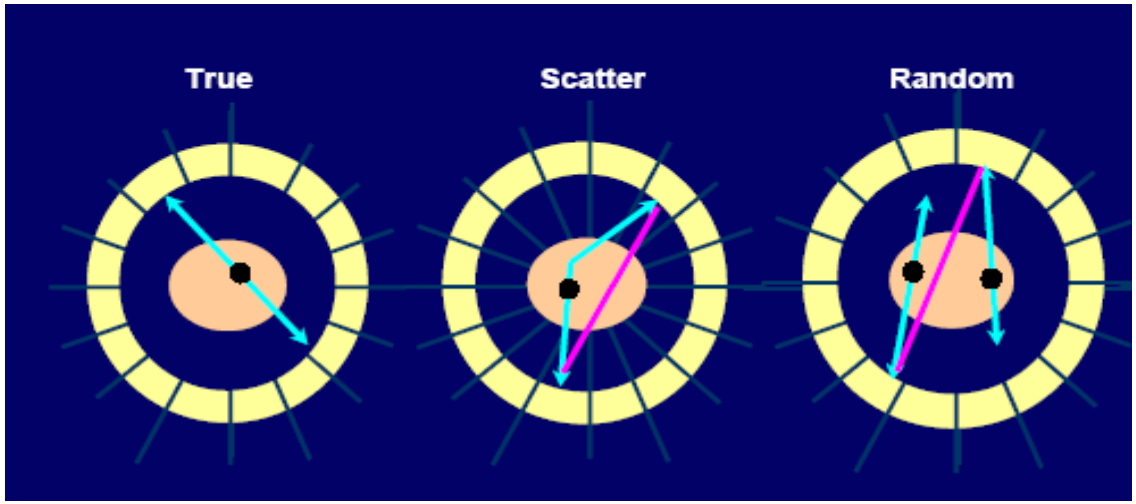

The noise equivalent count rate (NEC) was introduced.
The NEC is defined as:

$$NEC = T^2 / (T+R+2S)$$

where T is the true coincidence rate, R is the random coincidence rate, and S is the scatter coincidence rate. An NEC curve provides a statistic which shows the dependence of the increase in trues on increasing activity in the field of view, yet is penalized by scatter and randoms, which provide inaccurate positional information about the source distribution and therefore degrade image contrast and quality. Figure 8 shows the typical NEC curve for a BGO PET scanner in 2D and 3D modes of operation.

Spatial Resolution in PET

$$FWHM = 1.2\sqrt{(d/2)^2 + b^2 + (0.0022D)^2 + r^2 + p^2}$$

Crystal, Coding → Intrinsic; Non-colinearity; Positron range; Parallax error

1.2	:	degradation due to tomographic reconstruction
d	:	crystal size
b	:	systematic inaccuracy of positioning scheme (range: 0-2 mm)
D	:	coincident detector separation
r	:	effective source size, including positron range 0.55mm w/ ^{18}F)
p	:	Parallax error (radial elongation)

* Derenzo & Moses, "Critical instrumentation issues for resolution <2mm, high sensitivity brain PET", in Quantification of Brain Function, Tracer Kinetics & Image Analysis in Brain PET, ed. Uemura et al, Elsevier, 1993, pp. 25-40.

Commercial clinical PET

	CTI ECAT Exact (922)	CTI ECAT HR+	CPS Accel	GE Advance	GE Discovery LS PET/CT	GE Discovery ST PET/CT	C-PET	CPS BGO PET/CT	CPS LSO PET/CT	Philips Allegro/ Gemini PET/CT[a]
Crystal	BGO	BGO	BGO	BGO	BGO	BGO	NaI:Tl	BGO	LSO	GSO
No. crystal /block	8x8	8x8	8x8	6x6	6x6	6x6	N/A	8x8	8x8	22x29
Crystal size										
Transaxial (mm)	6.39	4.39	6.45	4.0	4.0	6.2	470	4.39	6.45	4
Radial (mm)	20	30.0	25	30.0	30.0	30.0	25.4	30.0	25	20
No. of rings	24	32	24	18	18	21	N/A	32	24	
Transaxial FoV (cm)	58.5	58.5	58.5	50	55	60	57.6	58.5	58.5	57.6
Coinc wind (ns)	12	12	6	12	12.5	11.7	8	12	6	8
E.wind. (keV)	350–650	350–650	350–650	300–650	300–650	300–650	435-665	350–650	350–650	
Sensitivity 2D trues, (kcps μCi−1 cc−1)										
	180	200	200	217	146	300	N/A	N/A	N/A	N/A
3D transaxial resolution (mm)										
FWHM 1 cm	6.0	4.6	6.3	5.1	4.8	6.2	5.7	4.5	6.3	4.8
FWHM 10 cm	6.7	5.4	6.8	6.0	5.4	7.0	5.7	5.6	7.4	5.9
Scatter 3D%	36	36	36	36	36	29	25	37	34	<30
R = T (kcps)	345	570	330 (HR)	486 (HS)	460 (HS)			679 (3D)		119 @ 0.24 mCi

John L. Humm et al.Eur J Nucl Med Mol Imaging (2003)

Standard PET Camera Performance

Assume Detector Contribution: 2 mm FWHM

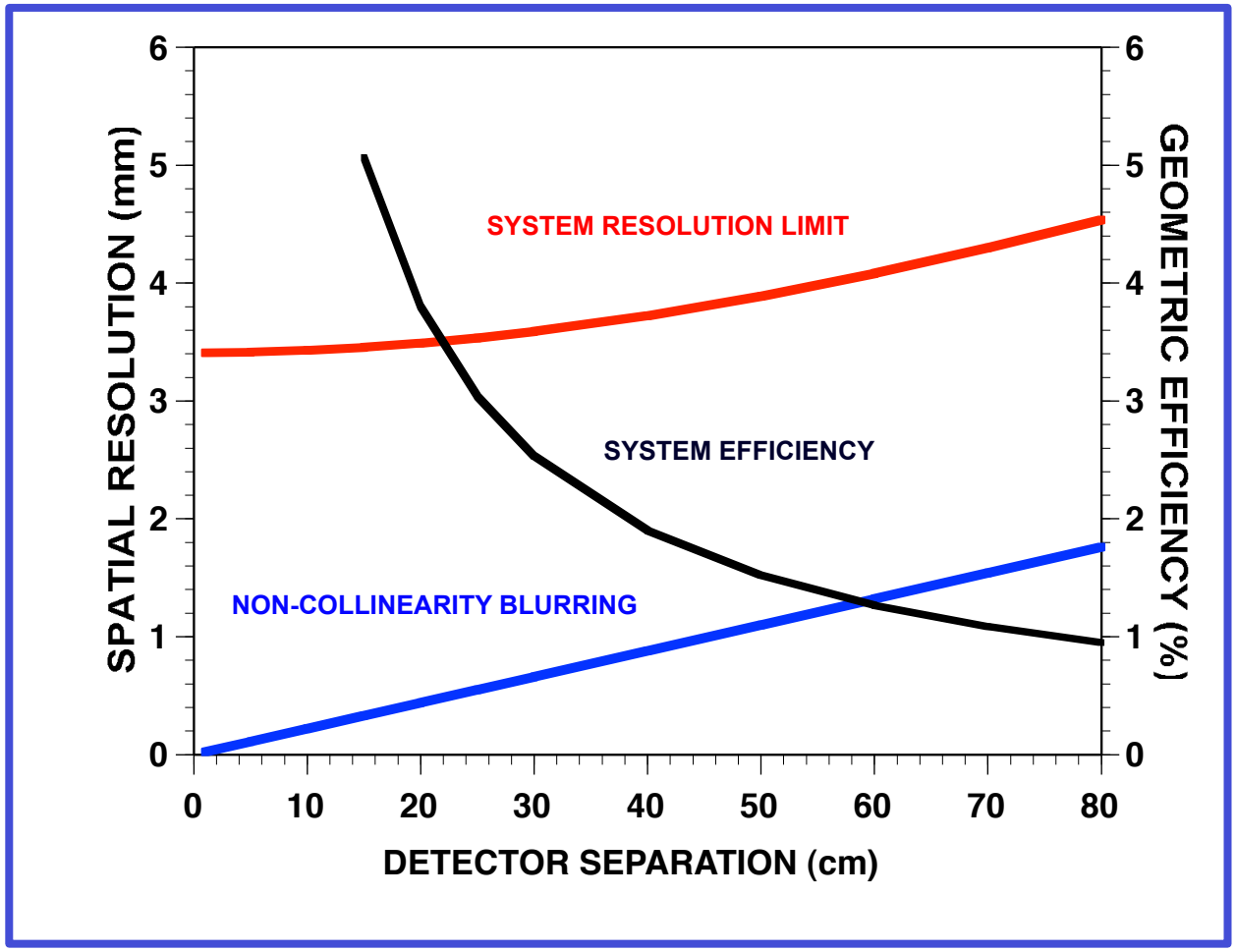

Small FoV PET has the best performances :
ideal for small animal Imaging

Courtesy of C. Levin Standford University

Intrinsic Spatial Resolution of PET Scanners

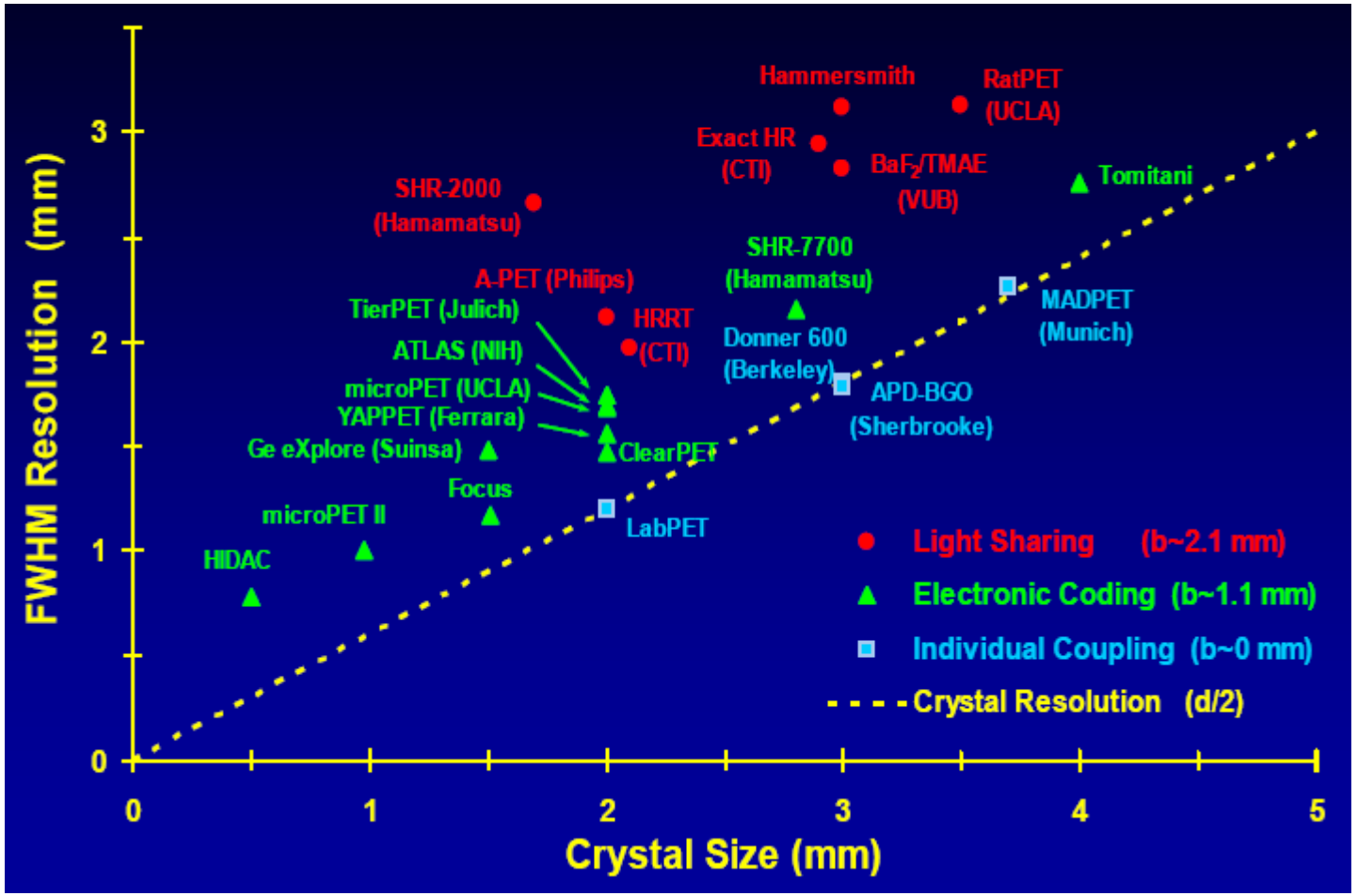

Courtesy of Roger Lecomte Sherbrooke University

… but small foV introduces Parallax error in PET

Depth of interaction (“DOI”)

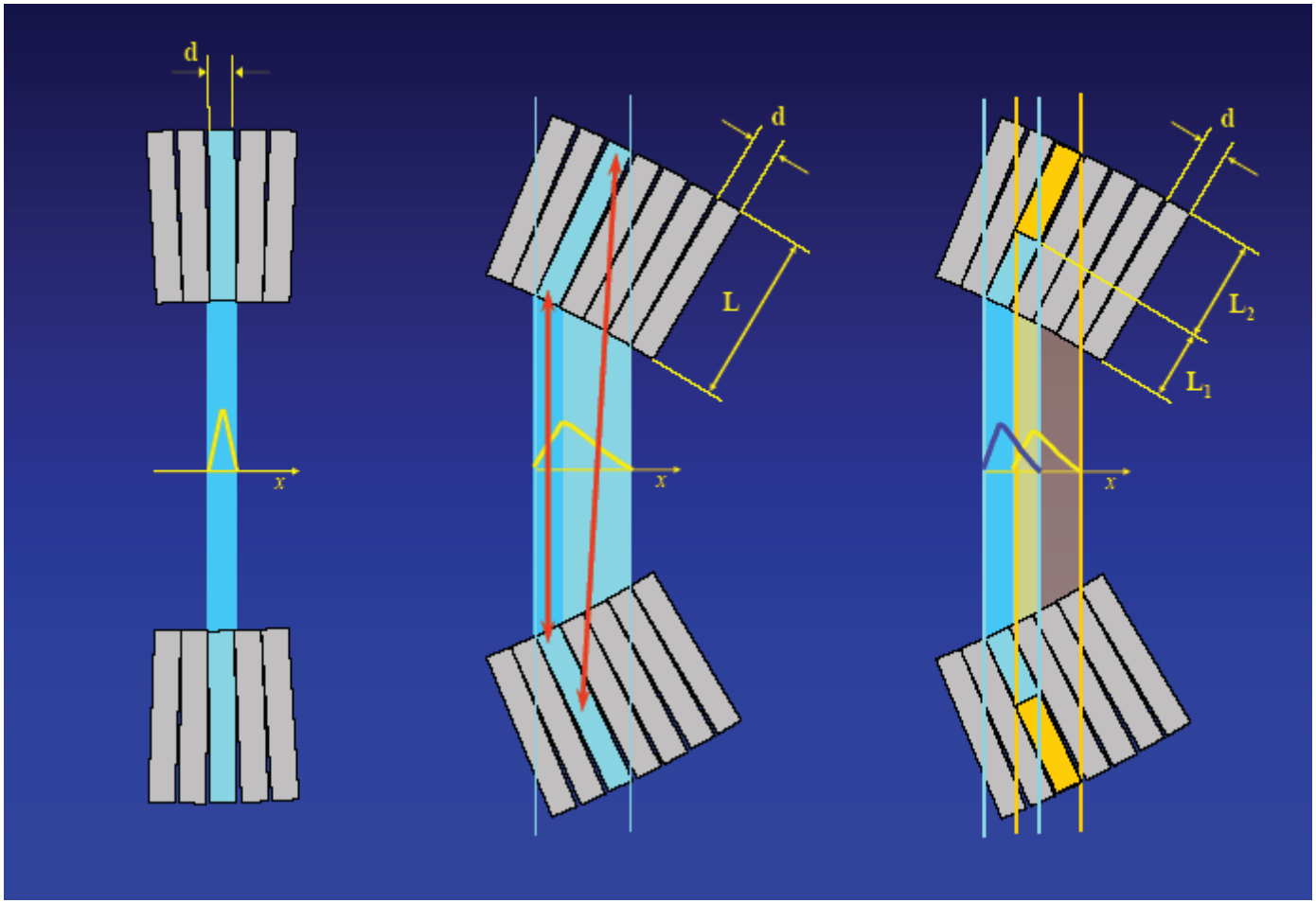

Courtesy of Roger Lecomte Sherbrooke University

Correction for DOI

-Pulse Height Discrimination (PHD) *(Rogers, IEEE TMI 14 (1995) 146-150)*
⇒*Sensitive to scatter (object & detector)*

-Light coding *(Thompsonet al, IEEE TNS 42 (1995) 1012-1017)*
⇒*Light loss causes degradation of resolution*

-Pulse Shape Discrimination (PSD) *(Lecomte, US Patent 1988)*
⇒*Insensitive to scatter, one readout channel per detector*
⇒*Requires scintillators with different decay times*

-Signal Ratio *(Huber et al, IEEE TNS 44 (1997) 1197-1201)*
⇒*Continuous measurement of DOI, not sensitive to scatter*
⇒*Requires 2 readout channels per detector (expensive)*

Future Perspective "fully 3D detector ……
"……1mm DOI resolution in PET ?

LaBr3:Ce continuous crystal

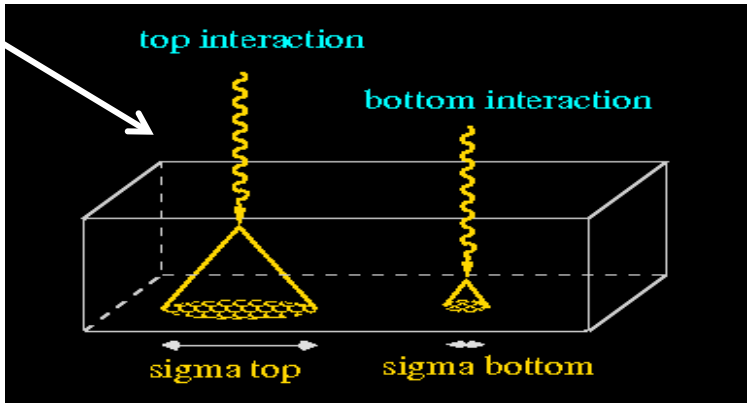

Preliminary results at 140 keV gamma ray energy

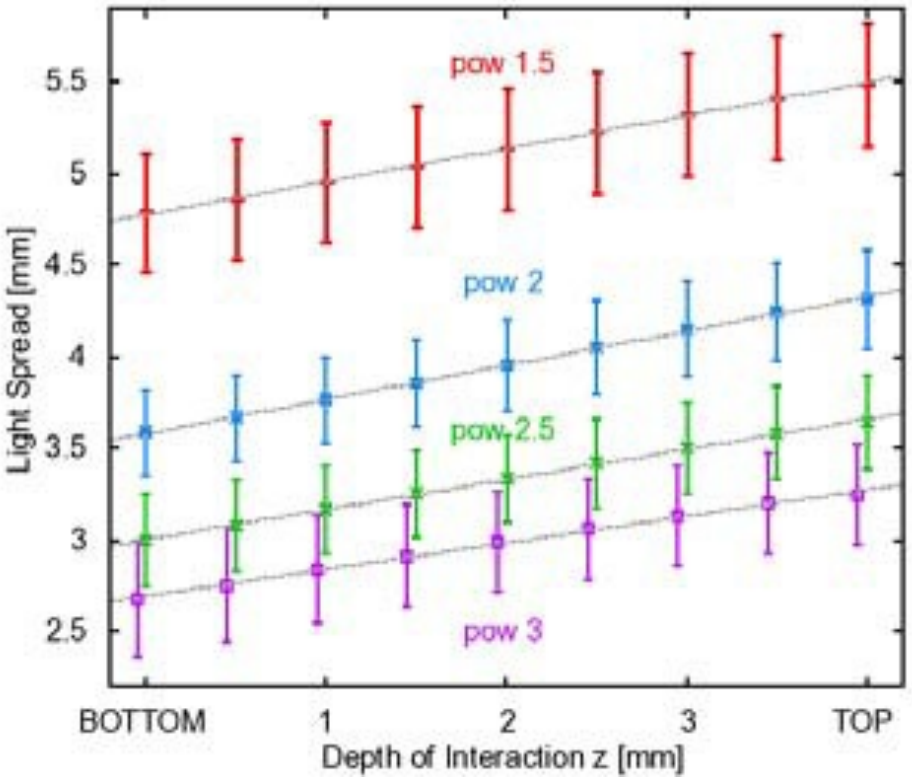

- ✓ Depth dependent response of continuous LaBr3:Ce crystals
- ✓ High photoelectron number reduces error on light spread discrimination

Investigation of depth dependent response of continuous LaBr3:Ce scintillation crystals

Pani, R.; Bennati, P.; Pellegrini, R.; Cinti, M.N.; Nourbakhsh, S. et al. Nuclear Science Symposium Conference Record (NSS/MIC), 2009 IEEE Publication Year: 2009 , Page(s): 3839

DoI position resolution in a continuous LaBr3(Ce) scintillation crystal for γ-ray imaging

Pani R., Nourbakhsh S., Pani P., Bennati P., Pellegrini R., Cinti M.N., et al. Nuclear Physics B (Proc. Suppl.) 215 (2011) 324–327

Depth of -Ray Interaction Within Continuous Crystals From the Width of Its Scintillation Light-Distribution

CWLerche, J. M. Benlloch, F. Sánchez, N. Pavón, B. Escat, E. N. Gimenez, M. Fernández, I. Torres, M. Giménez, A. Sebastià, and J. Martínez IEEE TRANSACTIONS ON NUCLEAR SCIENCE, VOL. 52, NO. 3, JUNE 2005

Depth of interaction decoding of a continuous crystal detector module

T Ling, T K Lewellen and R S Miyaoka Phys. Med. Biol. 52 (2007) 2213–2228

Parametric positioning of a continuous crystal PET detector with depth of interaction decoding

T Ling, T H Burnett, T K Lewellen and R S Miyaoka Phys. Med. Biol. 53 (2008) 1843–1863

Monolithic scintillator PET detectors with intrinsic depth-of-interaction correction

MC Maas, DR Schaart, DJ van der Laan, P Bruyndonckx, CLemaıtre, FJ Beekman and CWE van Eijk Phys. Med. Biol. 54 (2009) 1893–1908

Maximum-Likelihood Methods for Processing Signals From Gamma-Ray Detectors

H.H. Barrett, WC. J. Hunter, BW Miller, SK. Moore, Y. Chen, and L.R. Furenlid, IEEE TRANSACTIONS ON NUCLEAR SCIENCE, VOL. 56, NO. 3, JUNE 2009 725

Simultaneous microPET/CT Imaging

Goertzen, Meadors, Silverman, Cherry, Phys Med Biol 47; 4315-4328, 2002.

$^{18}F^-$ scan of mouse. 700 μCi injected
CT parameters: 40 kVp, 0.6 mA.
Data collected over 400 views in a time of 40 minutes.

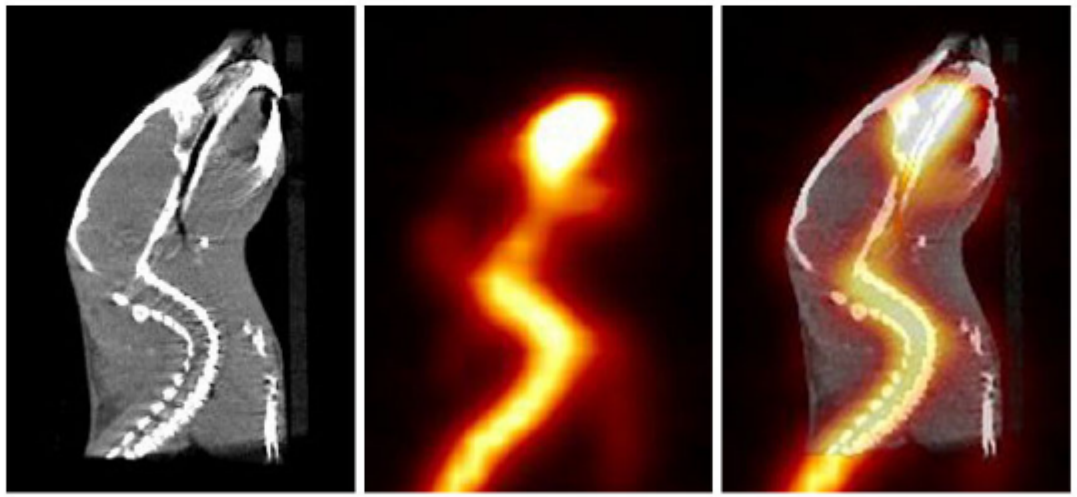

New PET scanners provide excellent sensitivity and spatial resolution of the order of 1-2 mm

New SPET scanners provide ultra high spatial Resolution (1 mm or better) at the cost of low sensitivity and a reduced field of view.

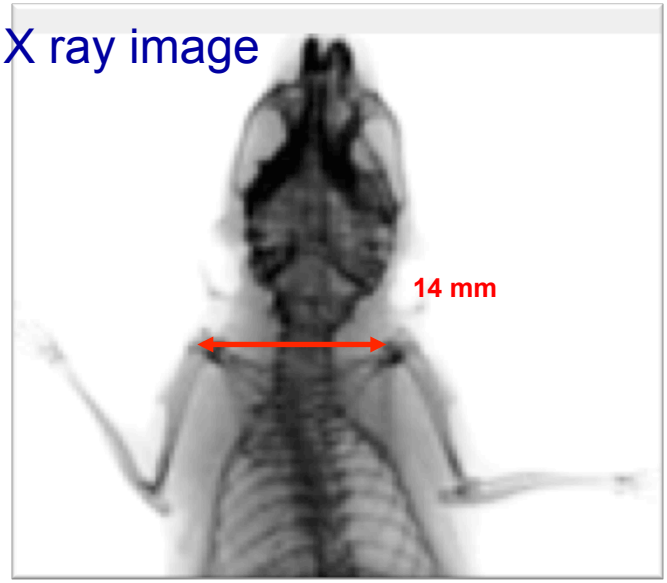

Mouse injected with ^{99m}Tc MDP

1 mm continuous NaI(Tl)
H9500 MA-PMT

Parallel Hole Collimator
(0.364 mm hole, 0.105 mm septa, 10.6 mm length)

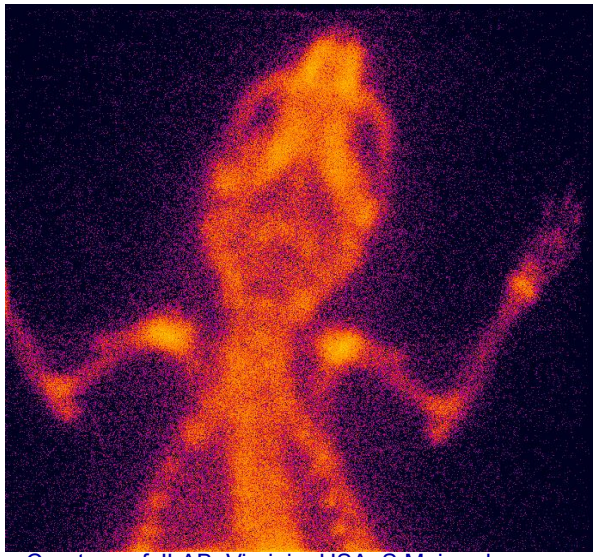

Courtesy of JLAB, Virginia, USA -S.Majewsky

10x20 cm^2 NaI(Tl) 1.2mm pitch pixellated modular detector

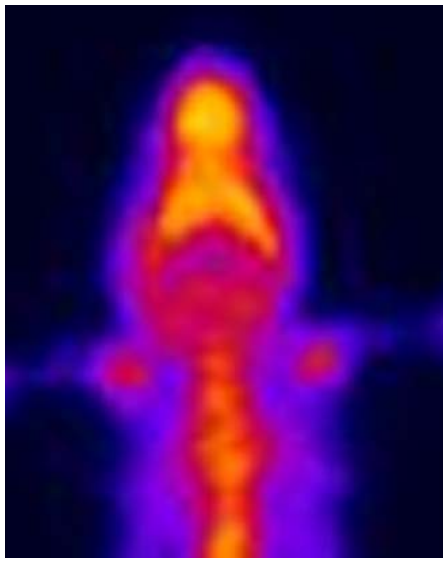

Parallel Hole Collimator

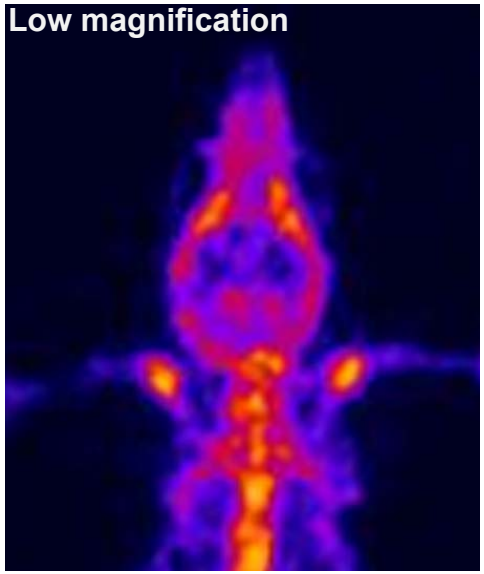

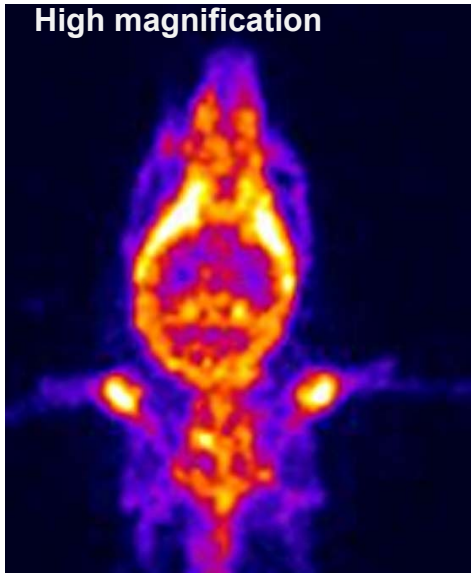

Pinhole Collimator

Courtesy of JHU
Maryland, USA
B.M.W.Tsui

Why TOF PET

Time resolution

⇩

Time of Flight information

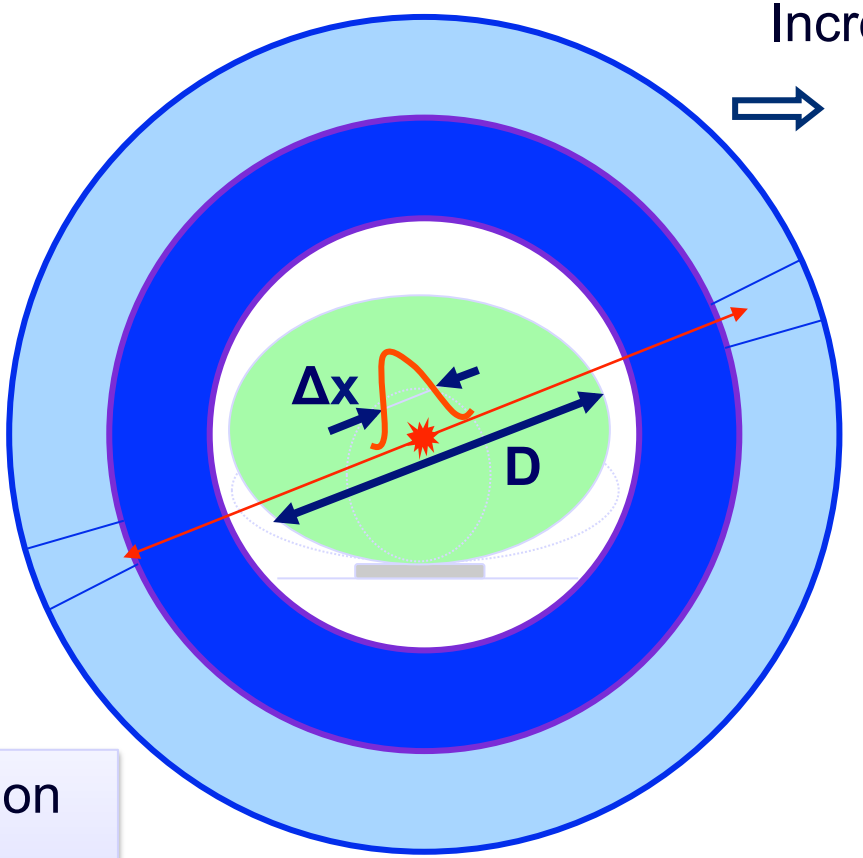

⇨ Increasing Obesity Background from Scattering!

Δx = uncertainty in position along LOR
= c · Δt/2

TOF 'Sensitivity' gain ~ D/Δx ⇨ Δt = 300 ps ⇨ Δx = 4.5 cm

> 5 x better Signal to Noise ratio

$LaBr_3$:Ce
Positron Emission Tomography

Full Module

1620 (60x27) 4mm x 4mm x 30mm $LaBr_3$:Ce crystals

10 PMTs - 50 mm diam - Raw Signals

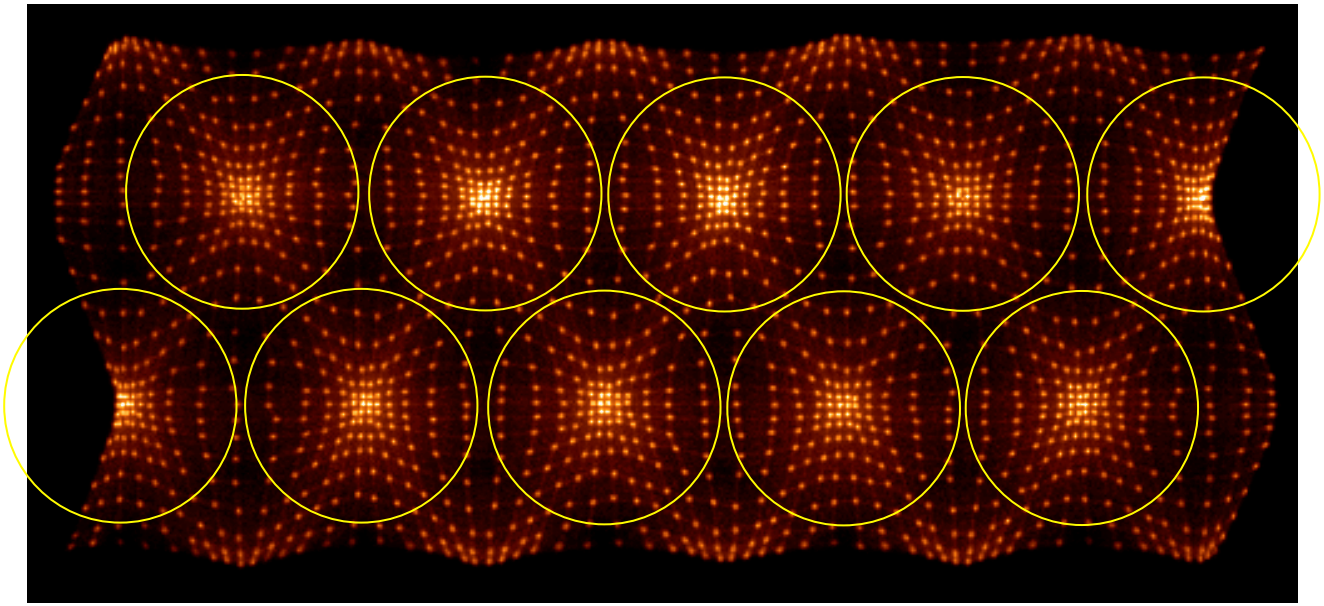

courtesy Philips Research Laboratories

$LaBr_3$:Ce (2001-2009) – 51 measurements

(all points are at 511 keV except cyan triangles that are at 1172 keV)

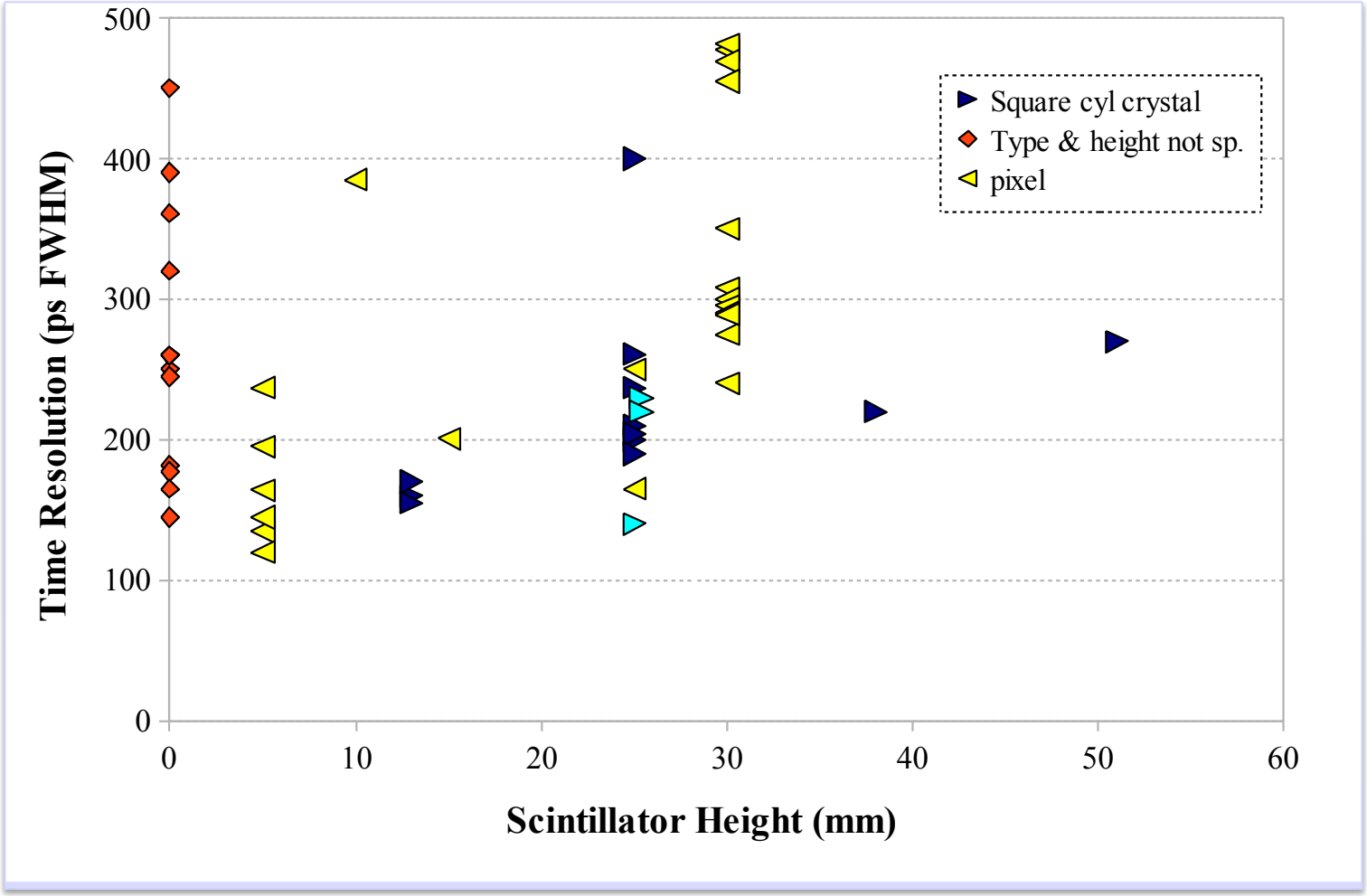

Code	Citation	Affiliations
P002	van Loef E.V.D., Dorenbos P., van Eijk C.W.E., Güdel H.U., Krämer K.W.; High-energy-resolution scintillator: Ce3 activated LaBr3; ApplPhysLett_79(2001)1573-1575	Delft Univ. (NL) and Bern Univ. (CH)
P052a	Shah K.S., Glodo J., Klugerman M., Moses W.W., Derenzo S.E., and Weber A.J.; LaBr3:Ce scintillators for gamma-ray spectroscopy; NSS-IEEE(2002)Vol.1_92-95. ALSO IN: TNS-IEEE_50(2003)2410–2413	Radiation Monitoring Devices Inc., Lawrence Berkeley National Laboratory (US)
P127a	Kuhn A., Surti S., Karp J.S., Raby P.S., Shah K.S., Perkins A.E., Muehllehner G.; Design of a lanthanum bromide detector for TOF PET; NSS-IEEE(2003)Vol.3_1953-1957. ALSO IN: TNS-IEEE_51(2004)2550-2557	Pennsylvania Univ., S.Gobain Crystals & Detectors, Radiation Monitoring Devices, Inc, Philips Medical Systems (US)
P058a	Glodo J., Moses W.W., Higgins W.M., van Loef E.V.D., Wong P., Derenzo S.E., Weber M.J., Shah K.S.; Effects of Ce concentration on scintillation properties of LaBr 3:Ce; NSS-IEEE(2004)Vol.2_998-1001. ALSO IN: TNS-IEEE_52(2005)1805-1808	Radiation Monitoring Devices Inc., Lawrence Berkeley National Laboratory (US)
P100a	Kuhn A., Surti S., Karp J.S., Muehllehner G., Newcomer F.M., van Berg R.; Performance Assessment of Pixelated LaBr3 Detector Modules for TOF PET; NSS-IEEE(2004)Vol.6_3402-3406. ALSO IN: TNS-IEEE_53(2006)1090-1095artno1645000	Pennsylvania Univ., Philips Medical Systems (US)
P023	Moses W.W., Shah K.S.; Potential for RbGd2Br7(Ce), LaBr3(Ce) and LuI3(Ce) in Nuclear Medical Imaging; NIMA_537(2005)317-320	Lawrence Berkeley National Laboratory, Radiation Monitoring Devices, Inc (US)
P074a	Nassalski A., Kapusta M., Batsch T., Wolski D., Moszynski M., Mockel D., Enghardt W.; Comparative Study of Scintillators for PET/CT Detectors; NSS-IEEE(2005)Vol.5_2823-2829artno1596921. ALSO IN: TNS-IEEE_54(2007)3-10	Soltan Institute for Nuclear Studies (PL), Forschungszentrum Rossendorf e.V. (DE)
P104	Kuhn A., Surti S., Shah K.S., Karp J.S.; Investigation of LaBr3 detector timing resolution; NSS-IEEE(2005)2022-2026artno1596730	Pennsylvania Univ., Radiation Monitoring Devices, Inc (US)
P027	Iltis A., Mayhugh M.R., Menge P., Rozsa C.M., Selles O., Solovyev, V.; Lanthanum halide scintillators: Properties and applications; NIMA_563(2006)359-363	Saint-Gobain Crystals (FR, US) and ENSCP (FR)
P029	C.M. Rozsa, M.R. Mayhugh, P.R. Menge, D. Rothan, C. Dathy; BrilLanCe® Scintillators LaCl3(Ce) and LaBr3(Ce), Recent Advances and Results; Presented at 2006 IEEE Nuclear Science Symposium; downloaded from www.detectors.saint-gobain.com on March 30, 2010.	Saint Gobain Crystals (FR)
P061	Moszynski M., Gierlik M., Kapusta M., Nassalski A., Szczesniak T., Fontaine Ch., Lavoute P.; New Photonis XP20D0 photomultiplier for fast timing in nuclear medicine; NIMA_567(2006)31-35	Soltan Institute for Nuclear Studies (PL) and Photonis (FR)
P045	Nicolini R., Camera F., Blasi N., Brambilla S., Bassini R., Boiano C., Bracco A., Crespi F.C.L., Wieland O., Benzoni G., Leoni S., Million B., Montanari D., Zalite A.; Investigation of the properties of a 1"x1" LaBr3:Ce scintillator; NIMA-582(2007)554-561	Milano Univ. and INFN (IT)
P065a	Swiderski L., Moszynski M., Nassalski A., Syntfeld-Kazuch A., Szczsniak T., Kamada K., Tsutsumi K., Usuki Y., Yanagida T., Yoshikawa A., and Chewpraditkul W.; Scintillation properties of praseodymium doped LuAG scintillator compared to cerium doped LuAG, LSO and LaBr3; NSS-IEEE(2008)2840-2846artno4774962. ALSO IN: TNS-IEEE_56-4(2008)2499-2505artno5204758	Soltan Institute for Nuclear Studies (PL), Materials Research Laboratory, Tohoku Univ. (JP), King Mongkut's Univ. (TH)
P075	Kyba C.C.M., Glodo J., van Loef E.V.D., Karp J.S., and Shah K.S.; Energy and Timing Response of Six Prototype Scintillators for TOF-PET; TNS-IEEE_55(2008)1404-1408artno454514	Pennsylvania Univ. and Radiation Monitoring Devices, Inc (US)
P118	Weisshaar D., Wallace M.S., Adrich P., Bazin D., Campbell C.M., Cook J.M., Ettenauer S., Gade A., Glasmacher T., McDaniel S., Obertelli A., Ratkiewicz A., Rogers A.M., Siwek K., Tornga S.R.; LaBr3:Ce scintillators for in-beam gamma-ray spectroscopy with fast beams of rare isotopes; NIMA_594(2008)56-60	Michigan Univ., Los Alamos National Laboratory (US)
P128	Schaart D.R., Seifert S., van Dam H.T., De Boer M.R., Vinke R., Dendooven P., Lohner H., Beekman F.J.; First experiments with LaBr3:Ce crystals coupled directly to silicon photomultipliers for PET applications; NSS-IEEE(2008)3991-3994artno4774157	Delft Univ., Groningen Univ . (NL)
P071	Kumar G.A., Mazumdar I., Gothe D.A.; Experimental measurements and GEANT4 simulations for a comparative study of efficiencies of LaBr3:Ce, NaI(Tl), and BaF2; NIMA_610(2009)522-529	Tata Institute of Fundamental Research (IN)
P073	Conti M., Eriksson L., Rothfuss H., Melcher C.; Comparison of fast scintillators with TOF PET potential; TNS-IEEE_56(2009)926-933	Siemens Molecular Imaging, Tennessee Univ. (US)

Dual-Modality PET/CT and SPET/CTImaging

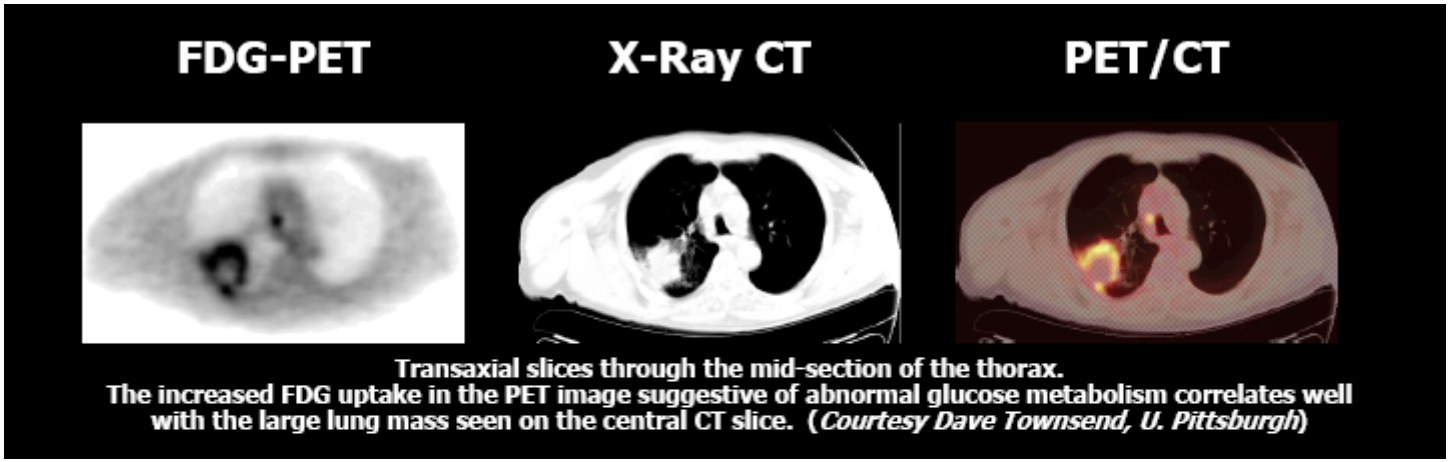

Radiation Dosimetry/Treatment Planning

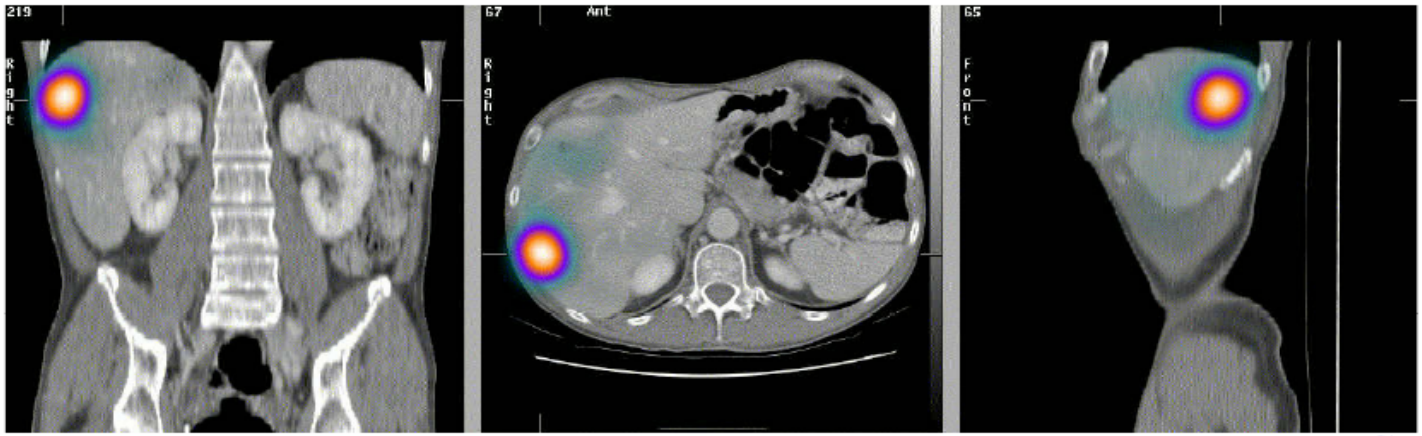

HERMES
HERMES MEDICAL SOLUTIONS

[^{131}I]-lipiodol therapy

INFN Ecorad Collaboration
US-SPET dual modality imager

❖ The ECORAD collaboration aims to develop a dual compact camera for acquiring ultrasound and scintigraphic images.

❖ It will allow to get both morphological and functional information on the same device. A volumetric image containing the fusion information will be provided to the user

•Small FoV gamma cameras improve visual quality by a closer positioning to the object

•Radionuclide imaging intrinsically lacks anatomic cues that are needed to localize or stage disease and typically has poorer statistical and spatial characteristics than anatomic imaging methods.

•Functional and anatomic information need to be considered together if one wants to give meaning to a small photon emission image and obtain a more reliable diagnosis.

•Ultrasounds are a cost-effective and reliable method.

•Ultrasound probes are one of the most common ways to assemble portable devices.

ECORAD US-SPET dual modality imager

Integrated system for morphological and functional imaging

Images reconstruction geometry gamma and 3D US

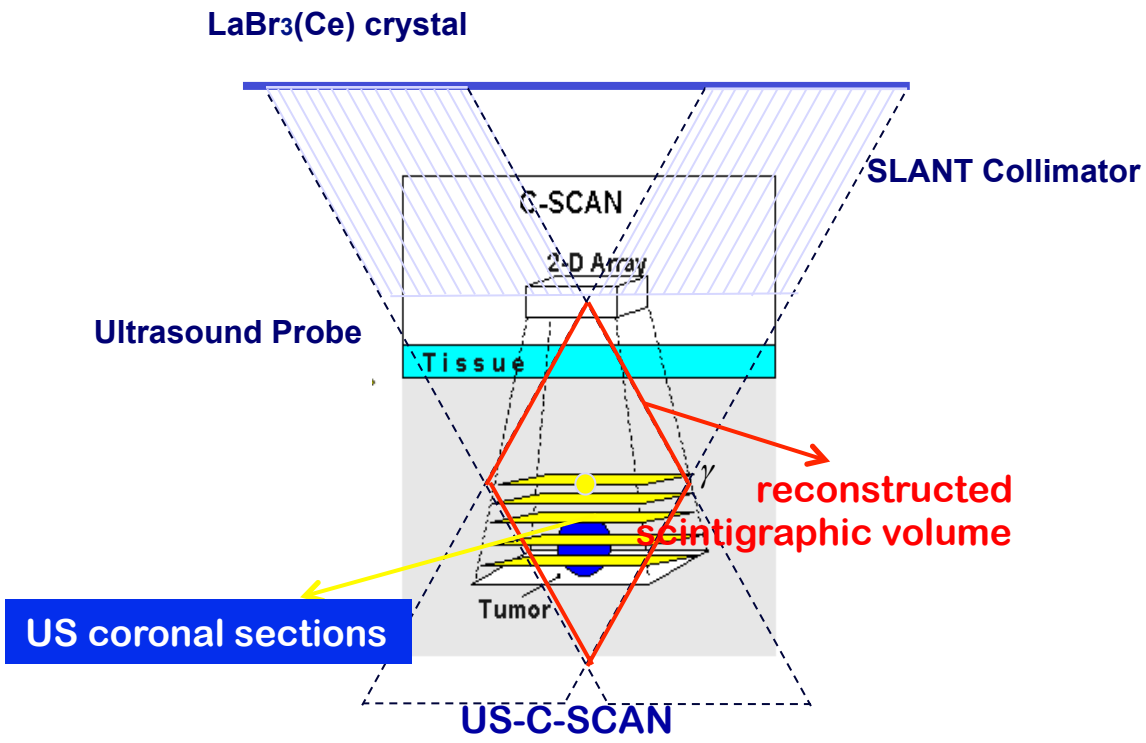

Four slants collimators rotating around the object with stationary gamma camera

Stationary 3D SPET gamma camera

TOP view

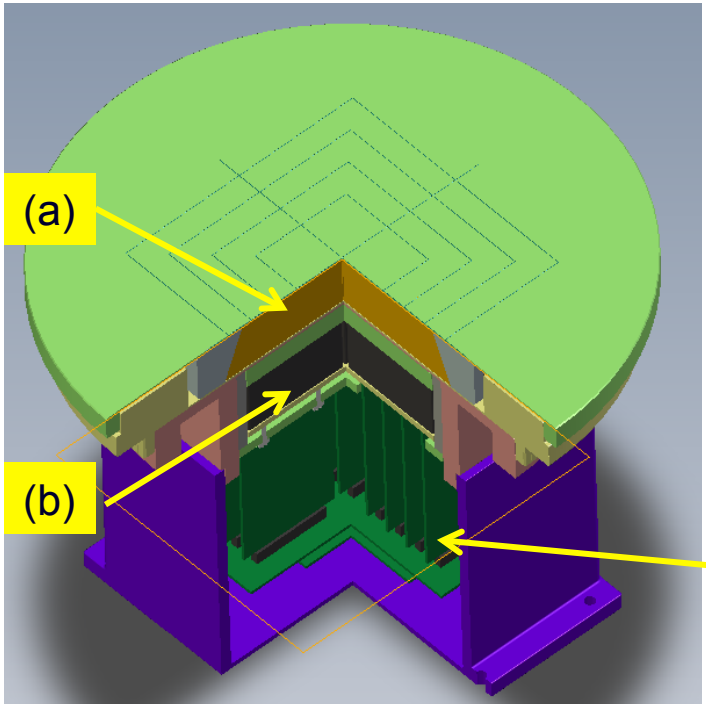

Side view

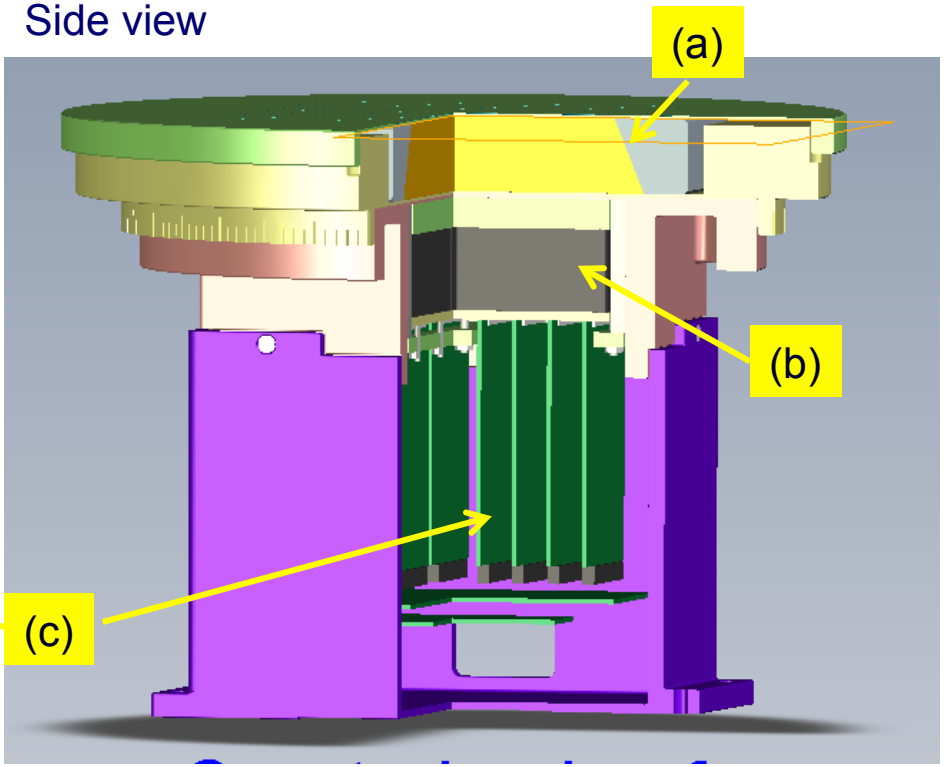

a) Slant-hole collimator
b) LaBr3 scintillation detector
c) 256ch electronics read-out

Sketch of the slant collimators

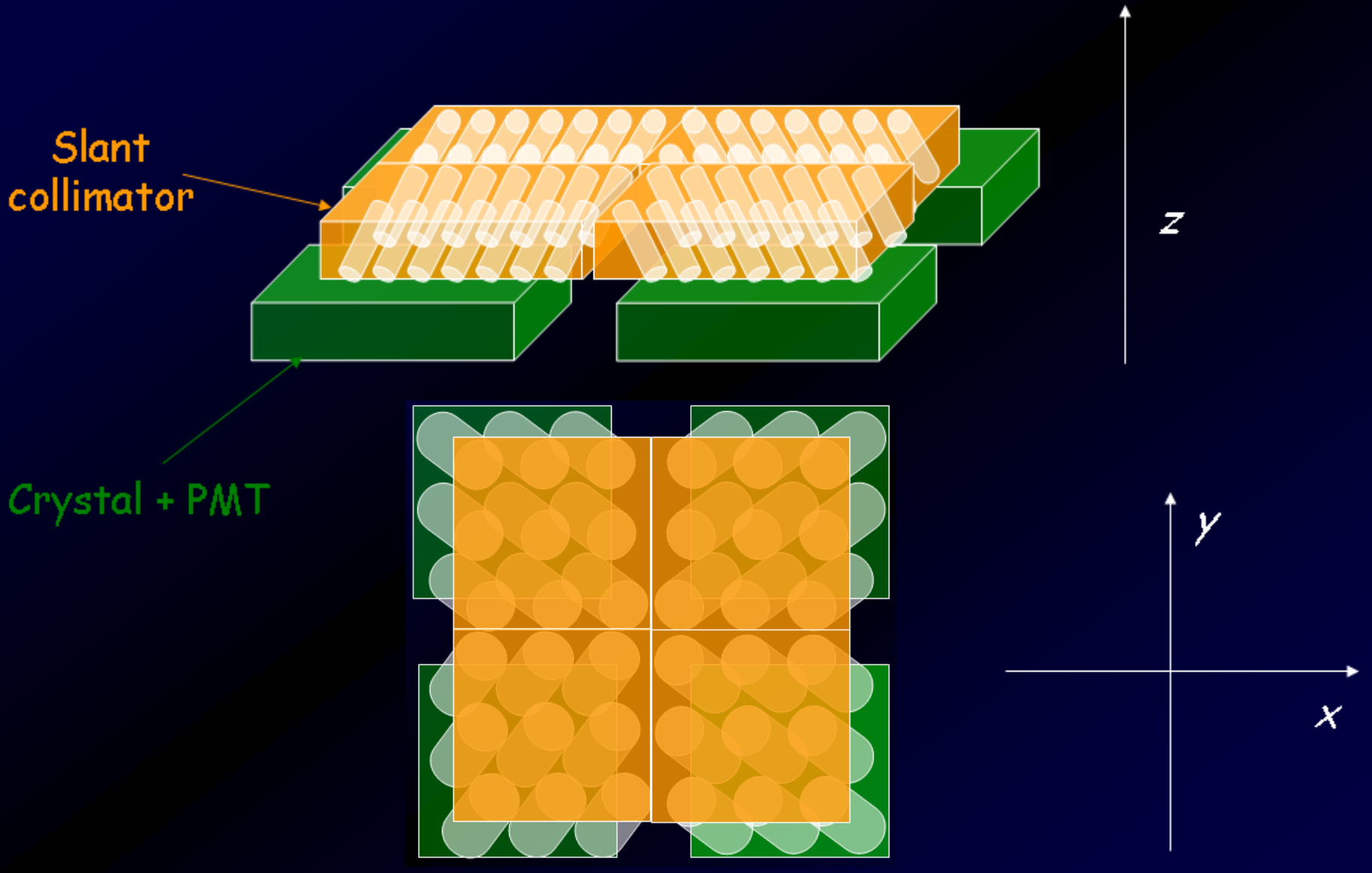

3D gamma Tomo-syntesis

Calibration Test object:

- 6 mm Ø diameter disk (10 µl)
- Filled with 50 µCi of Tc^{99m}
- Placed at 45 mm from collimator

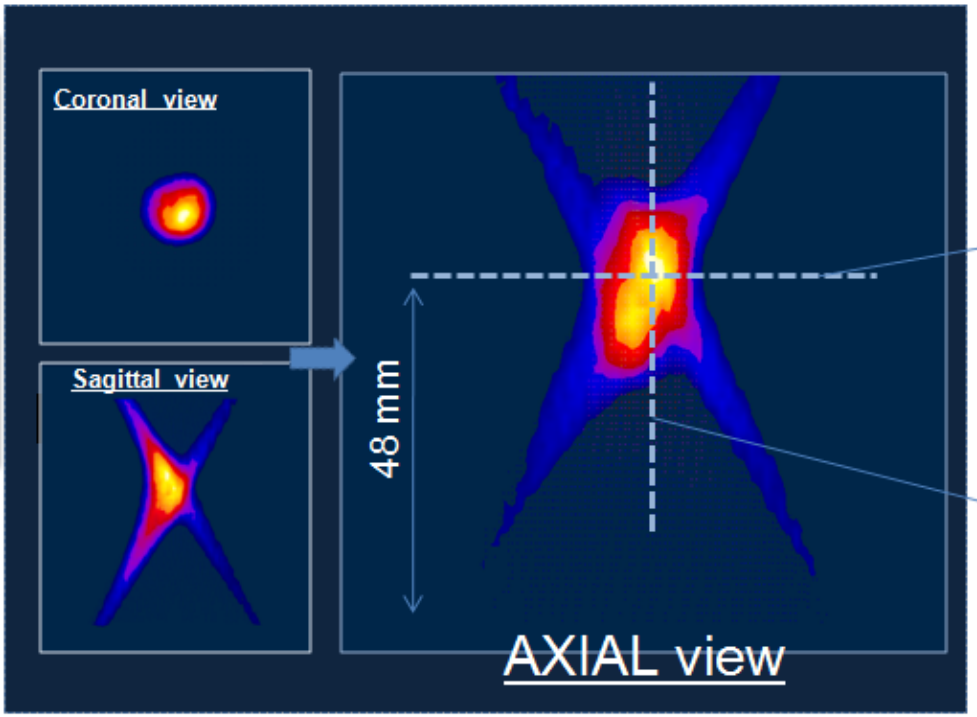

Coronal Plane

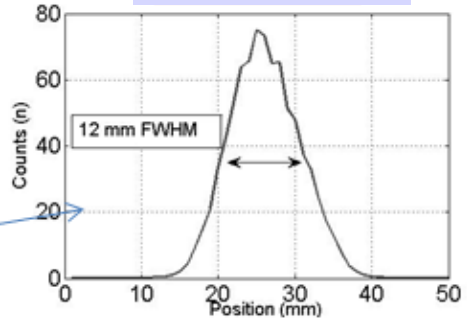

Axial Plane

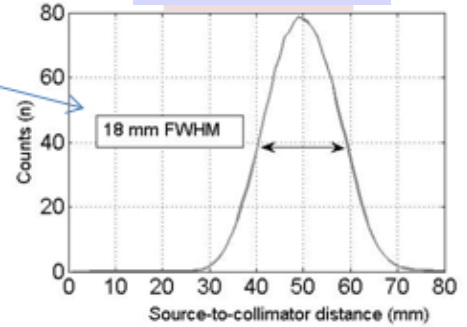

Results	Planar SR	Depth SR
MC	7 mm	12-14 mm
Planar Gamma	~ 8 mm	-
3D gamma	10 mm	18 mm

Conclusion:

- Good axial position determination
- coronal SR results 30% worst than MC
- Image artifacts due to the collimator angle

“Biological” Experiment

Quail egg

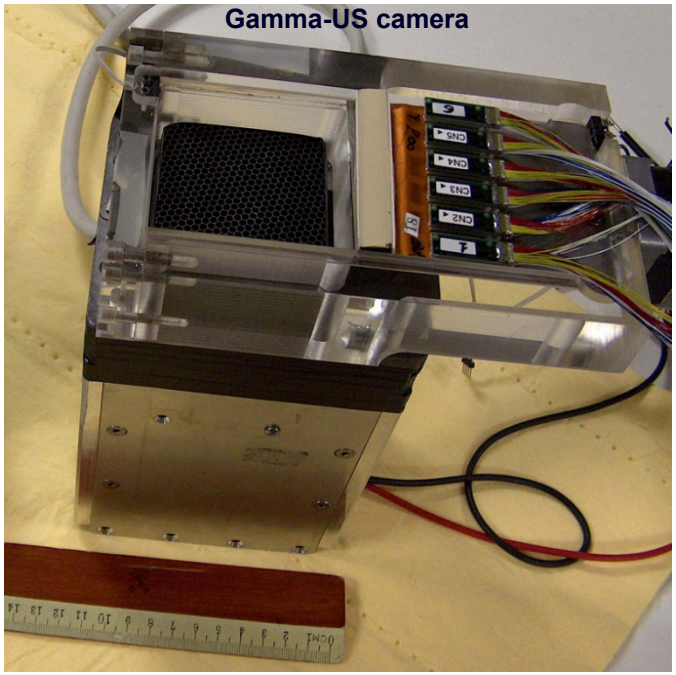

Small FoV
gamma camera

Phantom

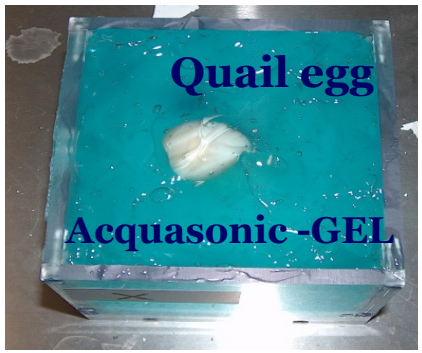

Front view

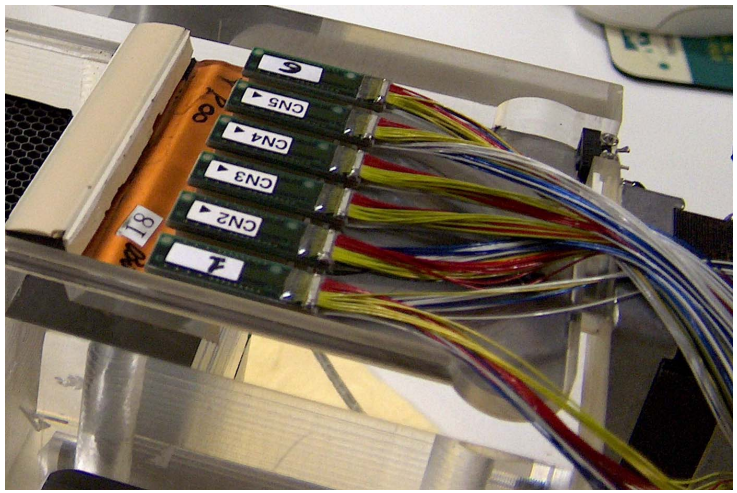

US probe

US and Scintigraphic images : 3D US & 2D Gamma

US Image 1mm SR

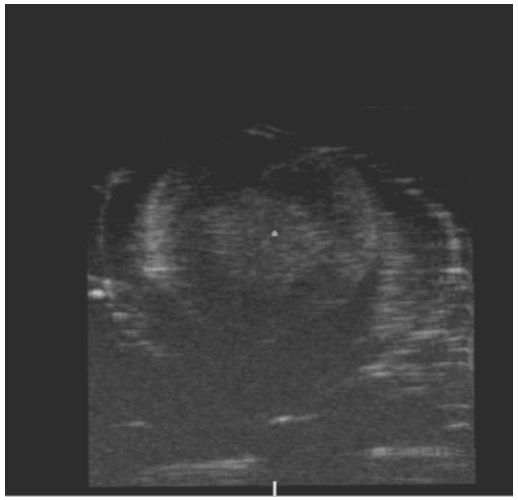

Scintigraphy 2 mm SR

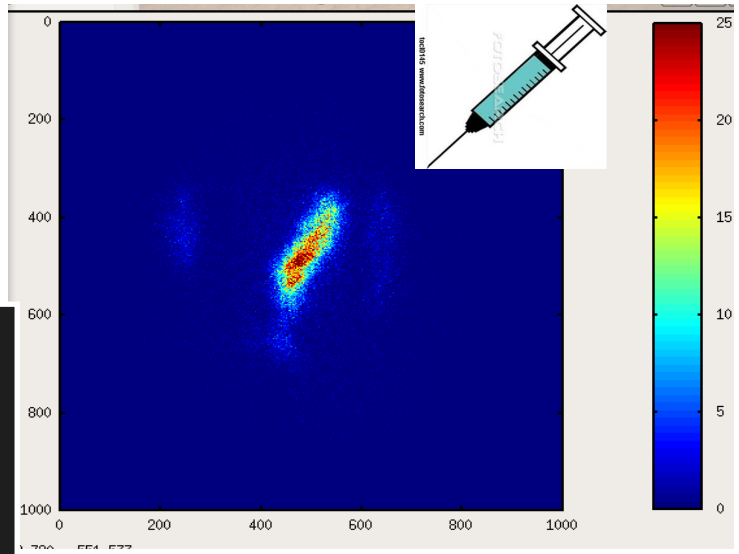

US-Scintigraphy dual image:

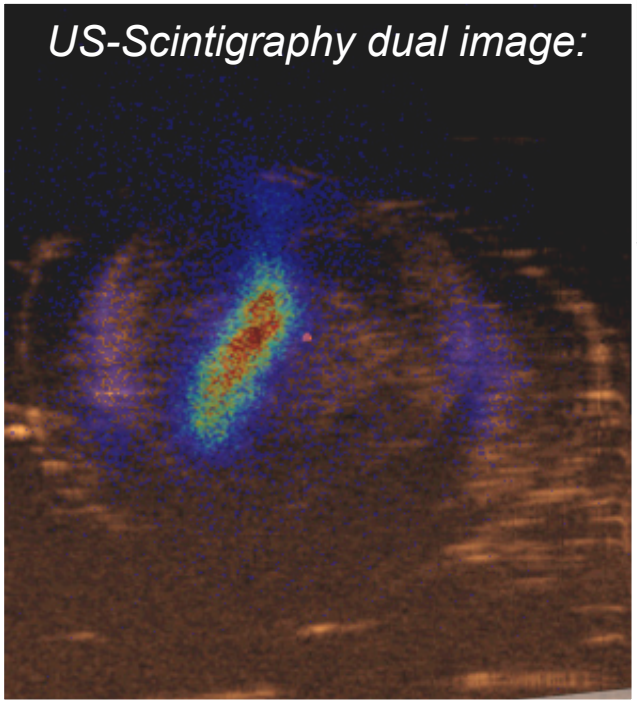

Egg after injection
(20 µl Tc99m + methylene blue

Conclusioni

Sfide future in SPET e PET

- ✓ Cristalli continui per rivelatori SPET e PET ad alta risoluzione spaziale.
- ✓ Cristalli continui per SPET 3D per applicazioni cliniche con collimatori slant.
- ✓ Cristalli continui per DOI in PET per applicazioni cliniche con piccoli anelli ed imaging biologico
- ✓ Cristalli continui per SPET con risoluzioni spaziali radiologiche per applicazioni SPET/CT a rivelatore unico
- ✓ Gamma Camere di piccolo campo combinate con sistemi di imaging anatomico (dual imaging)
- ✓ Tomografia SPET i piccoli organi basata su camere statiche e collimatori paralleli obliqui. (eliminazione dei grandi anelli)